HELMHOLTZ ZENTRUM DRESDEN ROSSENDORF

Pion parton distribution functions and transverse momentum dependent distribution functions

Minghui Ding

Helmholtz-Zentrum Dresden-Rossendorf, Institute of Theoretical Physics, Dresden, Germany

September 22, 2023

Workshop on parton distribution functions at a crossroad, September 18-22, 2023, ECT*, Italy.

The pion

Naive picture:
up quark + down antiquark:

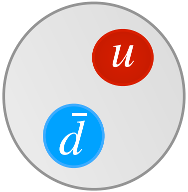

Realistic picture:
up quark + down antiquark + sea quarks + gluons

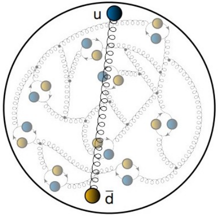

Nambu-Goldstone bosons of spontaneously broken chiral symmetry.

Mass: ~ 140 MeV; the lightest hadron; spin 0; P parity $-$; pseudoscalar meson.

Nambu-Goldstone boson

Pion does not fit naturally into the mass pattern typical of constituent quark model:

Maris, Roberts, Tandy, Phys. Lett. B 420 (1998) 267-273.

$$f_\pi m_\pi^2 = 2 m_u \rho_\pi \tag{1}$$

f_π, leptonic decay constant; m_π, pion mass; m_u, current quark mass; ρ_π, pseudoscalar projection of the pion wave function onto the origin in configuration space.

- Gell-Mann-Oakes-Renner (GMOR) relation
- Pion mass m_π vanishes in the absence of current quark mass m_u - Nambu-Goldstone boson of chiral symmetry breaking (When current quark mass is zero, QCD Lagrangian possesses a chiral symmetry).
- Mass square of pion rises linearly with the current quark mass, $m_\pi^2 \propto m_u$, whereas in constituent quark model $m_{\text{meson}} \propto m_{\text{quark}}$.

Nambu-Goldstone boson

Axial-vector Ward-Takahashi identity in chiral limit: $\mathcal{M}^{ab} = 0$; anomaly: $\mathcal{A}^a(k;P) = 0$.

$$P_\mu \Gamma^a_{5\mu}(k;P) = \mathcal{S}^{-1}(k_+) i\gamma_5 \mathcal{F}^a + i\gamma_5 \mathcal{F}^a \mathcal{S}^{-1}(k_-) \tag{2}$$

Quark propagator: $S^{-1}(k) = i\gamma\cdot k A(k^2) + B(k^2)$, right hand side:

$$\lim_{P^2\to 0} R = i\gamma_5 B(k^2)\,, \tag{3}$$

Massless pion pole in axial vector vertex: $\Gamma_{5\mu}(k,P) \xrightarrow{P^2=-m_\pi^2} \frac{f_\pi P_\mu}{P^2+m_\pi^2}\Gamma_\pi(k;P)$, left hand side:

$$\lim_{P^2\to 0} L = i\gamma_5 f_\pi E_\pi(k;P=0)\,, \tag{4}$$

Compare Eq.(3) and Eq.(4)

$$f_\pi E_\pi(k;P=0) = B(k^2)\,. \tag{5}$$

Nambu-Goldstone boson

Pion's Goldberger-Treiman relation: Maris, Roberts, Tandy, Phys. Lett. B 420 (1998) 267-273.

$$f_\pi E_\pi(k; P = 0) = B(k^2) \tag{6}$$

Pion's Bethe-Salpeter amplitude, solution of the Bethe-Salpeter equation

$$\Gamma_\pi(k; P) = \gamma_5[iE_\pi(k; P) + \gamma\cdot PF(k; P) + \gamma\cdot kk\cdot PG(k; P) + \sigma_{\mu\nu}k_\mu P_\nu H(k; P)] \tag{7}$$

Dressed-quark propagator

$$S^{-1}(k) = i\gamma\cdot kA(k^2) + B(k^2) \tag{8}$$

Dynamical chiral symmetry breaking (DCSB) $\Leftrightarrow$ Goldstone theorem

- Pion exists if, and only if, mass is dynamically generated
- Algebraically explain why pion is massless in the chiral limit
- Two body problem is solved, almost completely, once solution of one body problem is known

One-Body Matter Sector

Two body problem is solved, almost completely, once solution of one body problem is known. Quark propagator:

$$S(k;\zeta) = \frac{1}{i\gamma\cdot kA(k^2;\zeta) + B(k^2;\zeta)} = \frac{Z(k^2;\zeta)}{i\gamma\cdot k + M(k^2)} \tag{9}$$

- Massless partonic quarks acquire a momentum dependent mass function which is large at infrared momenta.
- This mass scale is responsible for all hadron masses.
- Properties of the nearly massless pion are the clearest window onto emergence of hadron mass (EHM) in the Standard Model.

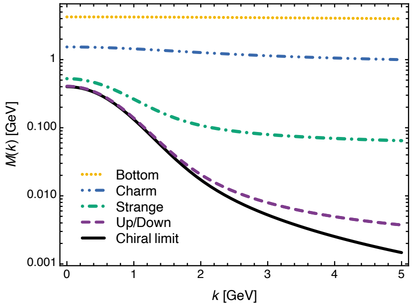

Roberts, Richards, Horn, Chang, Prog. Part. Nucl. Phys. 120 (2021) 103883.

The structure of pion

Form factor: the closest thing we have to a snapshot, the size, shape and makeup of pion

- Electromagnetic form factor
- Two-photon transition form factor
- Gravitational form factor

1D picture of how quarks move within pion

- Parton distribution amplitude
- Parton distribution function (PDF)

A multidimensional view of pion structure

- Transverse momentum dependent distribution function (TMD)
- Generalized parton distribution (GPD)

Part I

Parton distribution function (PDF)

Pion parton distribution function

Parton distribution function

- Probability densities: describe the light-front fraction, x, of hadron's total momentum, carried by a given parton species within pion.

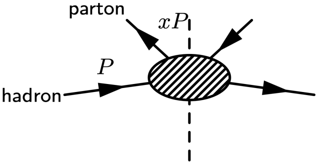

Four scenarios: (pion in isospin symmetry)

a quark; quark + antiquark; quark bound antiquark; QFT: $g \to q + \bar{q}$, etc.

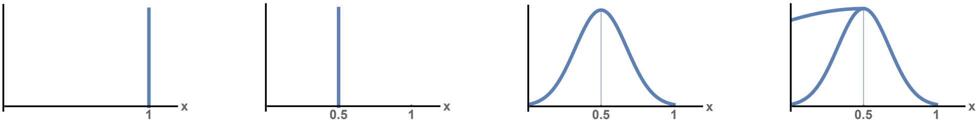

Pion parton distribution function

Synergy

- Experiments:
  - In the past: awarded a high priority – Led to
    (i) the discovery of quarks;
    (ii) Nobel prizes for the experiment leaders;
    (iii) the development of quantum chromodynamics (QCD)
  - Ongoing and in plan:
    Programmes at JLab, COMPASS++/AMBER; (cf. Oleg Denisov's talk)
    Proposals at EIC and EicC. (cf. Rong Wang's talk)
- Global fits: (cf. Aurore Courtoy's talk)
  Inferred from data, results viewed as benchmarks (JAM18, JAM21, xFitter, *Fantômas*, etc.)
- Continuum methods and Lattice QCD:(cf. Jianhui Zhang's talk)
  Historically, yielded only low-order Mellin moments. Pointwise behavior was not accessible.

Experiments on pion DF

- Valence distribution: (cf. Andrieux Vincent's talk)
  - Pion-induced Drell-Yan: $\pi^- N \to \mu^+ \mu^- X$;
    Past: CERN: NA3 (1983), NA10 (1985), Omega (1980); FNAL: E615 (1989);
    Future: COMPASS++/AMBER Phase-1 at CERN
  - Leading Neutron DIS: $ep \to e' n X$, Sullivan process;
    Past: HERA: ZEUS (2002), H1 (2010)
    Future: The Electron Ion Collider (EIC) in USA and China
- Glue distribution:
  (cf. Stephane Platchkov and Daniele Binosi's talk)
  - Prompt photon production: $\pi^+ p \to \gamma X$;
    Past: CERN NA24 (1987), WA70 (1988)
  - J/ψ production: $\pi^+ p \to J/\psi\ X$;
    Past: CERN: NA3 (1983)
    Future: COMPASS++/AMBER
- Sea distribution: momentum sum rule.
  - Future: COMPASS++/AMBER , with π^- and π^+ beams.

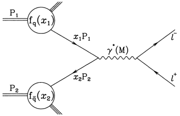

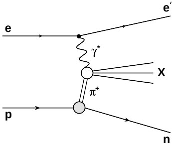

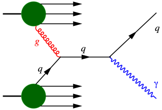

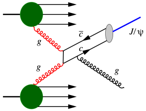

HZDR

Pion parton distribution function

Theoretical framework in continuum Schwinger function methods

- Concept (I): at a hadron scale ζ_H, dressed valence-quarks carry all the pion's light-front momentum and the glue and sea distributions vanish (Ding, Raya, Binosi, Chang, Roberts, Schmidt, Phys. Rev. D 101 (2020) 5, 054014)

$$\mathfrak{u}^\pi(1-x,\zeta_H) = \mathfrak{u}^\pi(x,\zeta_H) \tag{10}$$

- Numerically solve the bound-state equations to calculate valence distribution at hadron scale
- Concept (II): a proposition, there exists an effective charge, $\alpha_{1l}(k^2)$, that, when used to integrate the one-loop pQCD Dokshitzer-Gribov-Lipatov-Altarelli-Parisi (DGLAP) equations, defines an evolution scheme for parton PDFs that is all-orders exact. (Raya, Cui, Chang, Morgado, Roberts, Rodríguez-Quintero, Chin. Phys. C 46 (2022) 1, 013105. (cf. J. Rodríguez-Quintero's talk)

$$\frac{\langle x^n q^M\rangle_\zeta}{\langle x^n q^M\rangle_{\zeta_H}} = \exp\left[\frac{\gamma_0^n}{4\pi}\int_{\ln\zeta^2}^{\ln\zeta_H^2} d(\ln k^2)\,\hat{\alpha}(\ln k^2)\right] \tag{11}$$

- Evolve parton distribution function from hadron scale ζ_H to any other scale ζ.

Pion PDF at hadron scale

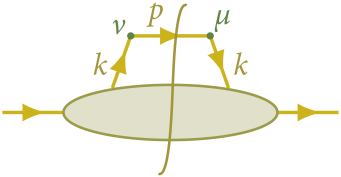

Leading-twist valence quark PDF in the operator representation:

$$q(x) = \frac{1}{4\pi} \int dz^- e^{-ixP^+ z^-} \langle P|\bar{\psi}(z^-) U^{-\dagger}_{(+\infty;z)} \gamma^+ U^-_{(+\infty;0)} \psi(0)|P\rangle \,, \tag{12}$$

Light-cone gauge: $n \cdot A = 0$, $U^{-\dagger}_{(+\infty;z)} = U^-_{(+\infty;0)} = 1$. In the parton model,

$$q(x) = \int \frac{d^4k}{(2\pi)^4} \delta\left(n{\cdot}k - xn{\cdot}P\right) \mathrm{Tr}\left[i\gamma{\cdot}n\, G(k,P)\right] . \tag{13}$$

Pion PDF at hadron scale

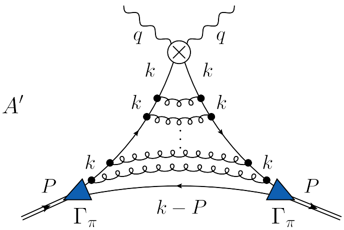

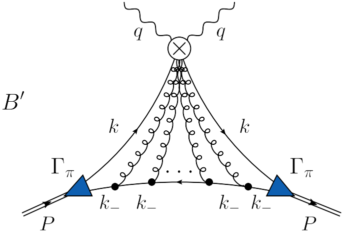

At hadron scale, dressed valence-quarks carry all the pion's light-front momentum, i.e., $\mathfrak{u}^\pi(1-x,\zeta_H) = \mathfrak{u}^\pi(x,\zeta_H)$. This relation is preserved only if both A' and B' diagrams are considered.

Chang, Mezrag, Moutarde, Roberts, Rodríguez-Quintero, Tandy, Phys. Lett. B 737 (2014) 23-29.

Pion PDF at hadron scale

$$q^\pi(x;\zeta_H) = N_c \mathrm{tr} \int_{dk} \delta_n^x(k_\eta)\; n\cdot\partial_{k_\eta} \left[\Gamma_\pi(k_\eta,-P;\zeta_H) S(k_\eta)\right] \Gamma_\pi(k_{\bar\eta},P)\, S(k_{\bar\eta})\,, \tag{14}$$

$S(k)$, quark propagator; $\Gamma_\pi(k,P;\zeta_H)$ pion Bethe-Salpeter amplitude.

Hadron scale
How to determine ζ_H?

At a hadron scale ζ_H, dressed valence-quarks carry all the pion's light-front momentum and the glue and sea distributions vanish. Ding, Raya, Binosi, Chang, Roberts, Schmidt, Phys. Rev. D 101 (2020) 5, 054014.

$$\mathfrak{u}^{\pi}(1-x,\zeta_H)=\mathfrak{u}^{\pi}(x,\zeta_H) \tag{15}$$

ζ_H is typically used as a parameter.

- A practitioner would develop a PDF model that is supposed to be valid at an unspecified scale, which is subsequently identified as ζ_H.
- Then a target PDF is identified, one that has typically been extracted through a phenomenological analysis of selected experimental data at experiment energy scale ζ_E.
- Finally chooses a value of ζ_H so that, after DGLAP evolution $\zeta_H \to \zeta_E$, the model PDF reproduces some property or properties of the target distribution at ζ_E.

Hadron scale - Process-independent (PI) effective charge

One-loop QCD running coupling

- $\alpha_{\overline{\text{MS}}}(k^2) = \frac{\gamma_m \pi}{\ln k^2/\Lambda^2_{\text{QCD}}}$
- Asymptotic freedom
- Landau pole ($k^2 = \Lambda^2_{\text{QCD}}$), coupling divergent

Process-independent effective charge

- Unique, nonperturbatively well-defined, calculable
- Large-k^2 behavior connects smoothly with one-loop QCD running coupling
- $\hat{\alpha}(k^2) = \frac{\gamma_m \pi}{\ln\left[\frac{\mathcal{K}^2(k^2)}{\Lambda^2_{\text{QCD}}}\right]}$, $\mathcal{K}^2(y = k^2) = \frac{a_0^2 + a_1 y + y^2}{b_0 + y}$ with (in GeV^2): $a_0 = 0.104, a_1 = 0.0975, b_0 = 0.121$.

  Cui et al., Chin. Phys. C 44 (2020) 8, 083102
- ...

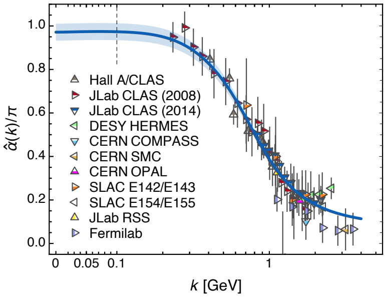

Binosi, Mezrag, Papavassiliou, Roberts, Rodríguez-Quintero, Phys. Rev. D 96, 054026 (2017).

Hadron scale - Process-independent (PI) effective charge

Absence of a Landau pole

- Owing to the appearance of a gluon mass scale
- Screening mass,
  $\zeta_H = \mathcal{K}(k^2 = \Lambda^2_{\text{QCD}}) \approx 1.4\Lambda_{\text{QCD}} \approx 0.331(2)$ GeV
  - $\sqrt{k^2} < \zeta_H$, the running slows
  - $\sqrt{k^2} < m_0/2$, the running ceases, effectively conformal, $m_0 = 0.43$ GeV
  - Deep infrared, saturates to $\hat{\alpha}(k^2 = 0) = \pi \times 0.97$
  - Gluons are screened, play no dynamical role
  - Valence quasiparticles carry all hadron properties at hadron scale ζ_H

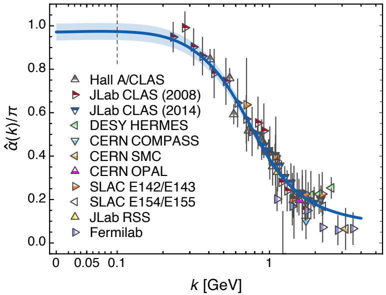

Match with the Bjorken process-dependent charge

- For practical intents and purposes, indistinguishable from process-dependent charge $\alpha_{g_1}(k^2)$, determined from the Bjorken sum rule

Infrared completion

- Effective charge at all accessible momentum scales, from the deep infrared to the far ultraviolet

Pion PDF at hadron scale

- Solid navy curve:
  $q^\pi(x;\zeta_H) = 213.32\,x^2(1-x)^2[1 - 2.9342\sqrt{x(1-x)} + 2.2911\,x(1-x)]\,,$
- long-dashed green curve:
  $q^\pi_{\tilde{\varphi}^2}(x;\zeta_H) = 301.66x^2(1-x)^2[1 - 2.3273\sqrt{x(1-x)} + 1.7889\,x(1-x)]^2\,.$
- Dotted black curve: scale free result
  $q_{\rm sf}(x) = 30x^2(1-x)^2$.
- A broad function, induced by dynamical chiral symmetry breaking.
- Large x behaviour: $q^\pi(x;\zeta_H) \sim (1-x)^2$.

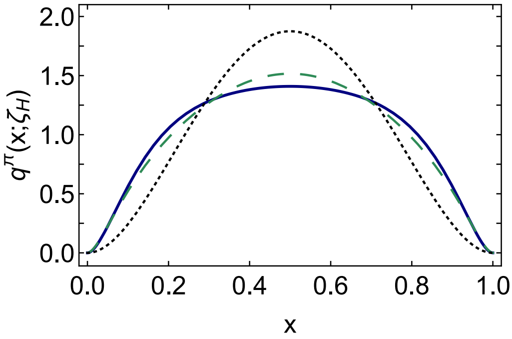

Pion PDF evolution

- GRS postulates that hadron DFs at a scale $\zeta_0^{\text{LO}} = 0.51$ GeV, evolving $q^\pi(x;\zeta_H) \to q^\pi(x;\zeta_0^{\text{LO}})$.
- Existing Lattice QCD calculations of low-order moments and phenomenological fits to pion parton distributions are typically quoted at $\zeta_2 = 2$ GeV, evolving $q^\pi(x;\zeta_H) \to q^\pi(x;\zeta_2)$.
- Experiment takes the average scale $\zeta_5 = 5.2$ GeV, evolving $q^\pi(x;\zeta_H) \to q^\pi(x;\zeta_5)$.
- Proposition: There exists an effective charge, $\alpha_{1l}(k^2)$, that, when used to integrate the one-loop pQCD DGLAP equations, defines an evolution scheme for parton PDFs that is all-orders exact. $\alpha_{1l}(k^2)$ need not be unique (We use process-independent charge here).

Valence quark distribution PDF Mellin moments: (Raya, Cui, Chang, Morgado, Roberts, Rodríguez-Quintero, Chin. Phys. C 46 (2022) 1, 013105.

$$\frac{\langle x^n q^M \rangle_\zeta}{\langle x^n q^M \rangle_{\zeta_H}} = \exp\left[\frac{\gamma_0^n}{4\pi}\int_{\ln \zeta^2}^{\ln \zeta_H^2} d(\ln k^2)\,\hat{\alpha}(\ln k^2)\right], \tag{16}$$

Sea quark and gluon PDF Mellin moments: (generated by valence PDF at hadron scale)

$$\begin{pmatrix} \langle x^n \rangle_\Sigma^\zeta \\ \langle x^n \rangle_g^\zeta \end{pmatrix} = \begin{pmatrix} \alpha_+^n S_-^n + \alpha_-^n S_+^n \\ \beta_{g\Sigma}^n \left(S_-^n - S_+^n\right) \end{pmatrix} \begin{pmatrix} \langle x^n \rangle_\Sigma^{\zeta_H} \\ 0 \end{pmatrix}. \tag{17}$$

Pion PDF at GRS scale $\zeta_0^{\text{LO}} = 0.51$ GeV

Continumm, Lattice and phenomenological fits - Mellin moments

	$\langle 2xu(x,\zeta_0^{\text{LO}})\rangle^{\pi}_{\text{valence}}$	$\langle xS(x,\zeta_0^{\text{LO}})\rangle^{\pi}_{\text{sea}}$	$\langle xG(x,\zeta_0^{\text{LO}})\rangle^{\pi}_{\text{gluon}}$
CSMs	0.73(7)	0.03(1)	0.24(5)
GRS	0.56	0.15	0.29

- valence-quark momentum fraction: GRS is $29(12)\%$ smaller than CSMs
- sea-quark momentum fraction: GRS is five-times greater than CSMs
- gluon momentum fraction: roughly comparable

GRS: M. Gluck, E. Reya, I. Schienbein, Eur. Phys. J. C 10, 313 (1999)

Pion PDF at GRS scale $\zeta_0^{\mathrm{LO}} = 0.51$ GeV

Continumm, Lattice and phenomenological fits - $x-$ profile

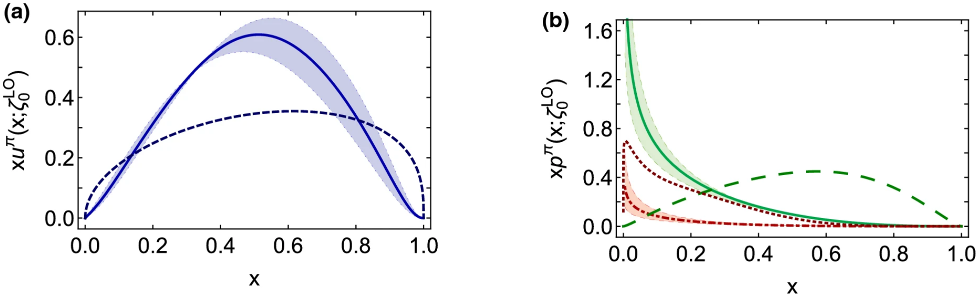

- valence-quark DF: GRS distribution is much harder than CSMs
- gluon DF: CSMs do not support the use of valence-like distributions for gluon at this scale.

Pion PDF at $\zeta_2 = 2$ GeV

Continumm, Lattice and phenomenological fits - Mellin moments

	$\langle x \rangle_u^\pi$	$\langle x^2 \rangle_u^\pi$	$\langle x^3 \rangle_u^\pi$
lQCD [53]	0.21(1)	0.16(3)	
lQCD [54]	0.254(03)	0.094(12)	0.057(04)
Ref. [102]	0.24	0.098	0.049
Refs. [39, 40]	0.24(2)	0.098(10)	0.049(07)
Herein	0.24(2)	0.094(13)	0.047(08)

- continuum and lQCD results agree on the light-front momentum fraction carried by valence-quarks in the pion $\langle 2xu(x,\zeta_2)\rangle^\pi_{\text{valence}} = 0.47(2)$.
- JAM18 analyzed data on π-nucleus Drell-Yan (DY) and leading neutron electroproduction and yielded $\langle 2xu(x,\zeta_2)\rangle^\pi_{\text{valence}} = 0.49(1)$, JAM18: P.C. Barry, N. Sato, W. Melnitchouk, C.-R. Ji, Phys. Rev. Lett. 121, 152001 (2018).
- sea-quark momentum fraction: CMS $\langle xS(x,\zeta_2)\rangle^\pi_{\text{sea}} = 0.11(2)$, JAM18 $\langle xS(x,\zeta_2)\rangle^\pi_{\text{sea}} = 0.16(1)$, CMSs is 30% smaller than JAM18.
- gluon momentum fraction: CMS $\langle xG(x,\zeta_2)\rangle^\pi_{\text{gluon}} = 0.41(2)$, JAM18 $\langle xG(x,\zeta_2)\rangle^\pi_{\text{gluon}} = 0.35(3)$, CMSs is 20% larger than JAM18.

Pion PDF at $\zeta_2 = 2$ GeV

Continumm, Lattice and phenomenological fits - Mellin moments

Resummation method	$\langle x \rangle_v$	$\langle x \rangle_s$	$\langle x \rangle_g$
NLO	0.53(2)	0.14(4)	0.34(6)
NLO + NLL cosine	0.47(2)	0.14(5)	0.39(6)
NLO + NLL expansion	0.46(2)	0.16(5)	0.38(6)
NLO + NLL double Mellin	0.46(3)	0.15(7)	0.40(5)

- JAM21 included various resummation prescriptions and yielded $\langle 2xu(x,\zeta_2)\rangle^{\pi}_{\text{valence}} = 0.46(3)$,

  JAM21: P.C. Barry, C.-R. Ji, N. Sato, W. Melnitchouk, Phys. Rev. Lett. 127 (2021) 23, 232001
- sea-quark momentum fraction: CMS $\langle xS(x,\zeta_2)\rangle^{\pi}_{\text{sea}} = 0.11(2)$, JAM21 $\langle xS(x,\zeta_2)\rangle^{\pi}_{\text{sea}} = 0.15(7)$, CMSs is 27% smaller than JAM21.
- gluon momentum fraction: CMS $\langle xG(x,\zeta_2)\rangle^{\pi}_{\text{gluon}} = 0.41(2)$, JAM21 $\langle xG(x,\zeta_2)\rangle^{\pi}_{\text{gluon}} = 0.39(6)$, CMSs is 5% larger than JAM21.

Pion PDF at $\zeta_2 = 2$ GeV

Continumm and phenomenological fits - $x-$ profile

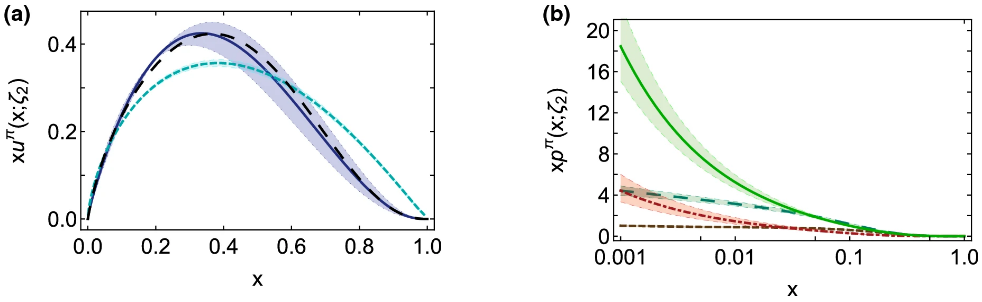

- Valence: x-profile is very different, JAM18 ignored NLL threshold resummation effects.

  Barry, Sato, Melnitchouk, Ji, Phys. Rev. Lett. 121, 152001 (2018). Cui et al., Eur. Phys. J. C 80, 1064 (2020).

- Glue: markedly different on $x \lesssim 0.05$. Sea: different on the entire x-domain.

Pion PDF at $\zeta_2 = 2$ GeV

Continuum and phenomenological fits - large x behaviour

QCD predicts large-x behavior of the valence-quark PDF:

$$q^{\Pi}(x;\zeta_H) \overset{x\simeq 1}{=} c(\zeta_H)\,(1-x)^{\beta_\Pi(\zeta_H)}\,, \tag{18a}$$

$$\beta_\Pi(\zeta_H) = 2\,, \tag{18b}$$

When evolved from ζ_H to ζ_E for comparison with experiment, the exponent $\beta_\Pi(\zeta_H)$ becomes $2+\gamma$, where the anomalous dimension $\gamma \gtrsim 0$ and increases logarithmically with ζ, so $q^{\Pi}(x;\zeta_E)$ must produce $\beta_\Pi > 2$.

Roberts, Richards, Horn, Chang, Prog. Part. Nucl. Phys. 120 (2021) 103883.

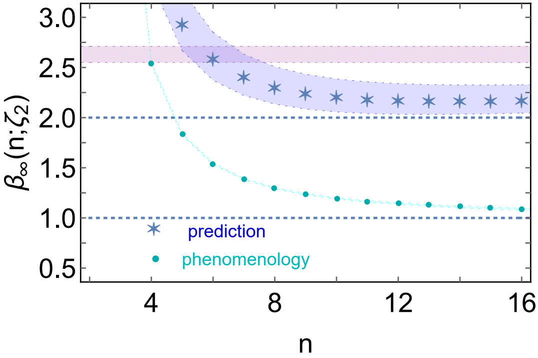

Pion PDF at $\zeta_2 = 2$ GeV

Continuum and Lattice - $x-$ profile

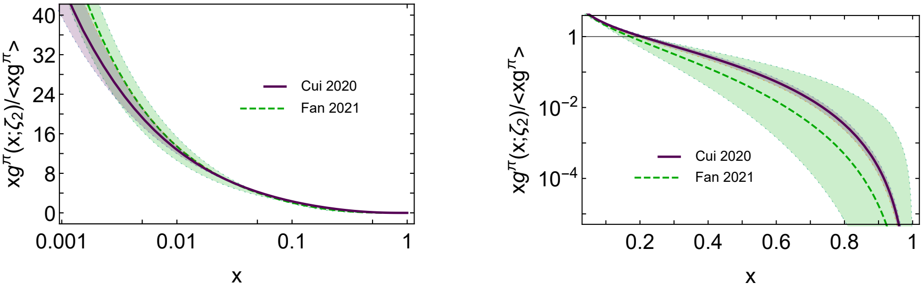

- Within uncertainties, there is point-wise agreement in pion glue distribution between the continuum and lattice on the entire depicted domains. Chang, Roberts, Chin. Phys. Lett. 38 (2021) 8, 081101.

Fan, Lin, Phys. Lett. B 823 (2021) 136778.

Pion PDF at $\zeta_5 = 5.2$ GeV

Continumm, Lattice and Experiment - Mellin moments

ζ_5	$\langle x \rangle_u^\pi$	$\langle x^2 \rangle_u^\pi$	$\langle x^3 \rangle_u^\pi$
Ref. [55]	0.18(3)	0.064(10)	0.030(5)
Herein	0.20(2)	0.074(10)	0.035(6)

- CSMs Mellin moments: $\langle 2xu^\pi(x;\zeta_5)\rangle = 0.41(4)\,,\ \langle x\rangle^\pi_{\text{sea}} = 0.14(2)\,, \langle x\rangle^\pi_g = 0.45(2)$.
- Text book result: on $\Lambda^2_{\text{QCD}}/\zeta^2 \simeq 0$, for any hadron, $\langle x\rangle_q = 0$, $\langle x\rangle_{\text{sea}} = 3/7 \approx 0.43$, $\langle x\rangle_g = 4/7 \approx 0.57$. There is a scale beyond which DFs cannot provide information that enables distinctions to be drawn between different hadrons: for each one, the valence distribution is a δ-function located at $x = 0$.

Pion PDF at $\zeta_5 = 5.2$ GeV

Continumm, Lattice and Experiment - $x-$ profile

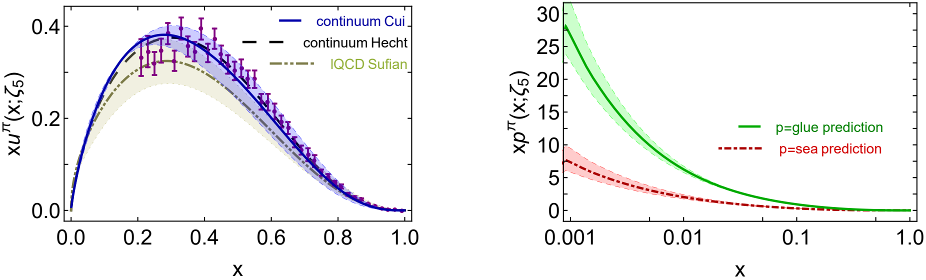

- Within uncertainties, continuum valence distribution (Cui) agrees with continuum in 2001 (Hecht), lattice (Sufian), and rescaled E615 experiment data. Conway et al.. Phys. Rev. D 39 (1989) 92-122. Hecht et al.. Phys. Rev. C 63, 025213 (2001). Aicher et al.. PRL 105, 252003 (2010). Sufian et al.. Phys. Rev. D 99, 074507 (2019). Cui et al., Eur. Phys. J. C 80, 1064 (2020).

Pion PDF at $\zeta_5 = 5.2$ GeV

Phenomenological fits

Phenomenological fits update PDFs by including NLL resummation effect.

- Double Mellin - does not yield appropriate PDFs at hadron scale.
- Mellin-Fourier - yield PDFs in agreement with $(1-x)^{\beta=2+\gamma}$ behavior at large x .

Barry, Ji, Sato, Melnitchouk, Phys. Rev. Lett. 127 (23) (2021) 232001. Cui et al. Eur. Phys. J. A 58 (2022) 1, 10.

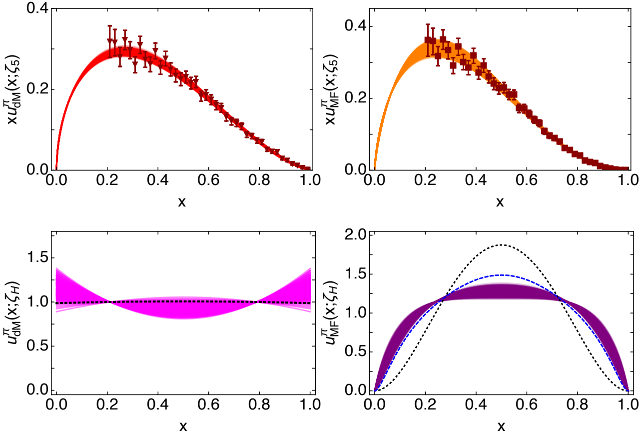

Pion PDF at $\zeta_5 = 5.2$ GeV

Continumm and Lattice

- Supposing only that there is an effective charge which defines an evolution scheme for PDFs that is all-orders exact, strict lower and upper bounds on all Mellin moments of the valence-quark PDFs of pion-like systems are derived.
- Lattice moments fall within the open band. Joó, Karpie, Orginos, Radyushkin, Richards, Sufian, Zafeiropoulos, Phys. Rev. D 100 (2019) 114512. Sufian, Karpie, Egerer, Orginos, Qiu, Richards, Phys. Rev. D 99 (2019) 074507. Alexandrou, Bacchio, Cloet, Constantinou, Hadjiyiannakou, Koutsou, Lauer, Phys. Rev. D 104 (5) (2021) 054504. Cui et al. Phys. Rev. D 105 (2022) 9, L091502.

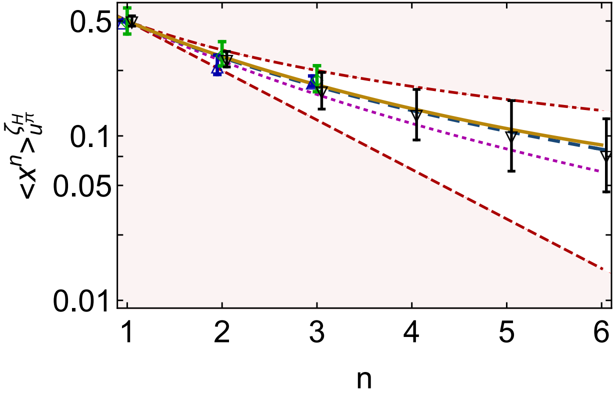

Pion PDF at $\zeta_5 = 5.2$ GeV

Continumm and Lattice

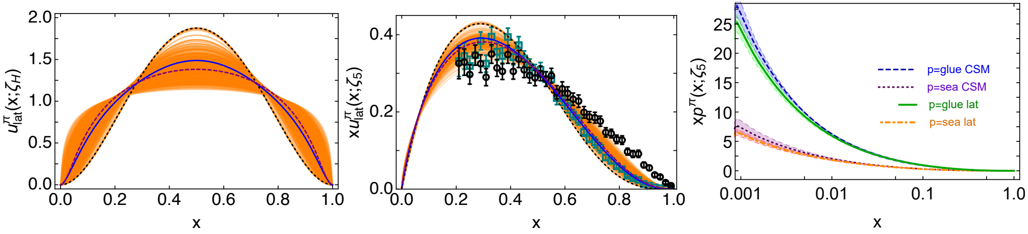

- Exploiting contemporary results from numerical simulations of lattice-regularised QCD, parameter-free predictions for pion valence, glue, and sea PDFs are obtained. Cui et al. Phys. Rev. D 105 (2022) 9, L091502.

Future facilities and experiments on pion PDFs

High Intensity, High Luminosity Facilities

- Jefferson Lab 22 GeV
- CERN: COMPASS++/AMBER
- Electron Ion Collider (EIC) in USA
- Electron-ion collider in China (EicC)

Jefferson Lab
Thomas Jefferson National Accelerator Facility

CERN

AMBER
A new QCD facility at the M2 beam line of the CERN SPS

Future Facilities and experiments on pion PDFs
Jefferson Lab 22 GeV

Tagged deep inelastic scattering (TDIS), Sullivan process

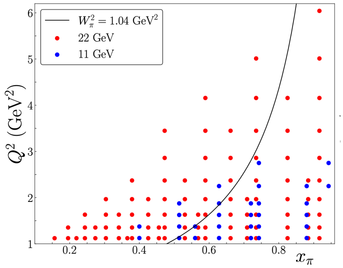

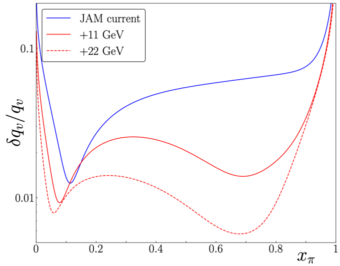

- JLab 22 GeV experiment offers a much larger phase space and x coverage (points located to the right of the curve $W_\pi^2 = 1.04$ GeV^2 will be eliminated).
- Relative uncertainty of the valence quark PDF is further reduced by inclusion of JLab 22 GeV pseudodata. JLab 22 GeV white paper.

Future Facilities and experiments on pion PDFs

COMPASS++/AMBER at CERN

AMBER at CERN - Apparatus for Meson and Baryon Experimental Research. Three phase-1 experiments:

- Proton charge-radius measurement using muon-proton elastic scattering
- Drell-Yan and J/ψ production experiments using the conventional M2 hadron beam
  - The structure of the pion: determination of the pion valence and sea-quark and gluon distributions
- Measurement of proton-induced antiproton production cross sections for dark matter searches.

Letter of Intent: A New QCD facility at the M2 beam line of the CERN SPS (COMPASS++/AMBER), arXiv:1808.00848 [hep-ex]. Proposal for Phase-1: COMPASS++/AMBER: Proposal for Measurements at the M2 beam line of the CERN SPS Phase-1: 2022-2024.

Program	Physics Goals	Beam Energy [GeV]	Beam Intensity [s^{-1}]	Trigger Rate [kHz]	Beam Type	Target	Earliest start time, duration	Hardware additions
muon-proton elastic scattering	Precision proton-radius measurement	100	$4 \cdot 10^6$	100	$\mu^\pm$	high-pressure H2	2022 1 year	active TPC, SciFi trigger, silicon veto,
Hard exclusive reactions	GPD E	160	$2 \cdot 10^7$	10	$\mu^\pm$	$NH_3^\uparrow$	2022 2 years	recoil silicon, modified polarised target magnet
Input for Dark Matter Search	$\overline{p}$ production cross section	20-280	$5 \cdot 10^5$	25	p	LH2, LHe	2022 1 month	liquid helium target
$\overline{p}$-induced spectroscopy	Heavy quark exotics	12, 20	$5 \cdot 10^7$	25	$\overline{p}$	LH2	2022 2 years	target spectrometer: tracking, calorimetry
Drell-Yan	Pion PDFs	190	$7 \cdot 10^7$	25	$\pi^\pm$	C/W	2022 1-2 years	
Drell-Yan (RF)	Kaon PDFs & Nucleon TMDs	$\sim$100	10^8	25-50	$K^\pm$, $\overline{p}$	$NH_3^\uparrow$, C/W	2026 2-3 years	"active absorber", vertex detector
Primakoff (RF)	Kaon polarisa-bility & pion life time	$\sim$100	$5 \cdot 10^6$	> 10	K^-	Ni	non-exclusive 2026 1 year	
Prompt Photons (RF)	Meson gluon PDFs	≥ 100	$5 \cdot 10^6$	10-100	$K^\pm$ $\pi^\pm$	LH2, Ni	non-exclusive 2026 1-2 years	hodoscope
K-induced Spectroscopy (RF)	High-precision strange-meson spectrum	50-100	$5 \cdot 10^6$	25	K^-	LH2	2026 1 year	recoil TOF, forward PID
Vector mesons (RF)	Spin Density Matrix Elements	50-100	$5 \cdot 10^6$	10-100	$K^\pm, \pi^\pm$	from H to Pb	2026 1 year	

Table 2: Requirements for future programmes at the M2 beam line after 2021. Muon beams are in blue, conventional hadron beams in green, and RF-separated hadron beams in red.

Future Facilities and experiments on pion PDFs

Electron Ion Collider (EIC) in USA

A machine for delving deeper than ever before into the building blocks of matter.

Sullivan process:

EIC Yellow Report, Nucl. Phys. A 1026 (2022) 122447.

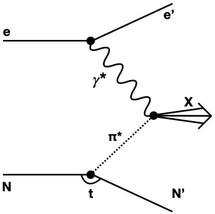

Table 7.1: Science questions related to pion and kaon structure and the understanding of the EHM mechanism accessible at the EIC, with the key measurements and some key requirements listed. Further requirements are addressed in the text.

Science Question	Key Measurement	Key Requirements
What are the quark and gluon energy contributions to the pion mass?	Pion structure function data over a range of x and Q^2.	• Need to uniquely determine $e+p \to e' + X + n$ (low $-t$) • CM energy range ~10-100 GeV • Charged and neutral currents desirable
Is the pion full or empty of gluons as viewed at large Q^2?	Pion structure function data at large Q^2.	• CM energy ~100 GeV • Inclusive and open-charm detection
What are the quark and gluon energy contributions to the kaon mass?	Kaon structure function data over a range of x and Q^2.	• Need to uniquely determine $e+p \to e' + X + \Lambda/\Sigma^0$ (low $-t$) • CM energy range ~10-100 GeV
Are there more or less gluons in kaons than in pions as viewed at large Q^2?	Kaon structure function data at large Q^2.	• CM energy ~100 GeV • Inclusive and open-charm detection
Can we get quantitative guidance on the emergent pion mass mechanism?	Pion form factor data for Q^2 = 10-40 $(\text{GeV}/c)^2$.	• Need to uniquely determine exclusive process $e+p \to e' + \pi^+ + n$ (low $-t$) • $e+p$ and $e+D$ at similar energies • CM energy ~10-75 GeV
What is the size and range of interference between emergent-mass and the Higgs-mass mechanism?	Kaon form factor data for Q^2 = 10-20 $(\text{GeV}/c)^2$.	• Need to uniquely determine exclusive process $e+p \to e' + K + \Lambda$ (low $-t$) • L/T separation at CM energy ~10-20 GeV • Λ/Σ^0 ratios at CM energy ~10-50 GeV
What is the difference between the impacts of emergent- and Higgs-mass mechanisms on light-quark behavior?	Behavior of (valence) up quarks in pion and kaon at large x.	• CM energy ~20 GeV (lowest CM energy to access large-x region) • Higher CM energy for range in Q^2 desirable
What is the relationship between dynamically chiral symmetry breaking and confinement?	Transverse-momentum dependent Fragmentation Functions of quarks into pions and kaons.	• Collider kinematics desirable (as compared to fixed-target kinematics) • CM energy range ~20-140 GeV
More speculative observables		
What is the trace anomaly contribution to the pion mass?	Elastic J/Ψ production at low W off the pion.	• Need to uniquely determine exclusive process $e+p \to e' + J/\Psi + \pi^+ + n$ (low $-t$) • High luminosity ($\geq 10^{34}\text{cm}^{-2}\,\text{sec}^{-1}$) • CM energy ~70 GeV
Can we obtain tomographic snapshots of the pion in the transverse plane? What is the pressure distribution in a pion?	Measurement of DVCS off pion target as defined with Sullivan process.	• Need to uniquely determine exclusive process $e+p \to e' + \gamma + \pi^+ + n$ (low $-t$) • High luminosity ($\geq 10^{34}\text{cm}^{-2}\,\text{sec}^{-1}$) • CM energy ~10-100 GeV
Are transverse momentum distributions universal in pions and protons?	Hadron multiplicities in SIDIS off a pion target as defined with Sullivan process.	• Need to uniquely determine SIDIS off pion $e+p \to e' + h + X + n$ (low $-t$) • High luminosity ($10^{34}\text{cm}^{-2}\,\text{sec}^{-1}$) • $e+p$ and $e+D$ at similar energies desirable • CM energy ~10-100 GeV

Future Facilities and experiments on pion PDFs

Electron-ion collider in China (EicC)

It will be constructed based on an upgraded heavy-ion accelerator, High Intensity heavy-ion Accelerator Facility (HIAF) which is currently under construction, together with a new electron ring.

Physics highlights:

- Partonic structure and three-dimensional landscape of nucleon
- Partonic structure of nuclei
- Exotic hadronic states
- Other important exploratory studies
  - Structure of light pseudoscalar mesons

EicC white paper, Front. Phys.(Beijing) 16 (2021) 6, 64701.

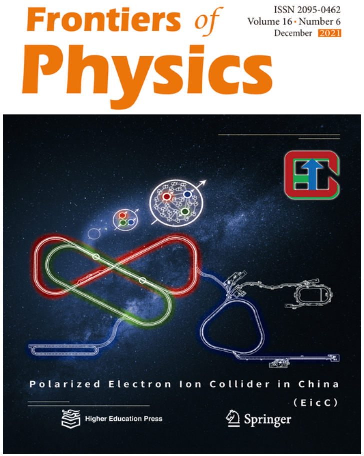

Part II

Transverse momentum dependent distribution function (TMD)

Transverse momentum dependent (TMD) distribution function

- Semi-inclusive deep inelastic scattering (SIDIS)

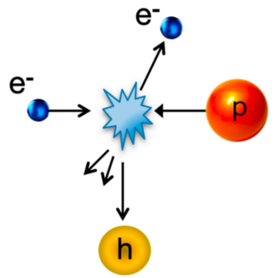

- Transverse momentum dependent (cf. Giovanni Salme's talk)

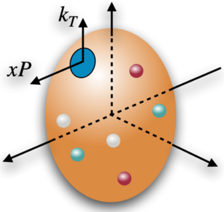

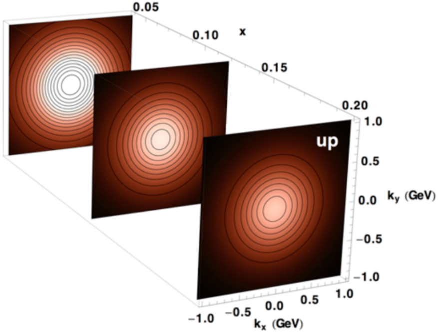

- Hadron tensor and correlation function
- Wilson line, process-dependent, not universal

Boer-Mulders function

quark pol.

nucleon pol.	U	L	T
U	f_1		$h_1^\perp$
L		g_{1L}	$h_{1L}^\perp$
T	$f_{1T}^\perp$	g_{1T}	$h_1,\ h_{1T}^\perp$

Twist-2 TMDs

- Transversely polarized quark in an unpolarized hadron
- Chiral odd
- Naive time-reversal odd
- SIDIS experiments such as ZEUS and H1 at DESY, e^+e^- annihilation experiments etc.

Correlation function

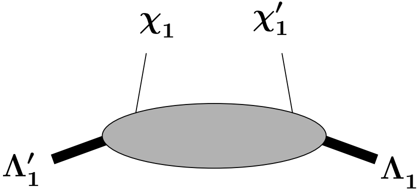

Figure: χ_1 and χ_1' are quark chirality, Λ_1' and Λ_1 are target hadron polarizations.

Correlation function $\Phi(p, P, S)$: a Dirac matrix depending on photon momentum p, target hadron momentum P and target hadron spin S, which can be decomposed as

$$\{p^\mu, P^\mu, S^\mu\} \otimes \{1, \gamma^5, \gamma^\mu, \gamma^\mu\gamma^5, \sigma^{\mu\nu}\}\,. \tag{19}$$

It satisfies the conditions of Hermiticity and parity invariance $(\bar{p} = (p^0, -\vec{p}))$ [Mulders, GGI lectures, 2015]:

$$\begin{aligned} \text{Hermiticity}: \quad & \Phi^\dagger(p, P, S) = \gamma^0 \Phi(p, P, S) \gamma^0\,, \\ \text{Parity}: \quad & \Phi(p, P, S) = \gamma^0 \Phi(\bar{p}, \bar{P}, -\bar{S}) \gamma^0\,. \end{aligned} \tag{20}$$

Correlation function for SIDIS

Integrated correlation function at leading twist for unpolarized target

$$\Phi(x, k_\perp) = \frac{1}{2} f_1(x, k_\perp)\gamma^- + \frac{i}{2} h_1^\perp(x, k_\perp) \frac{\not{k}_\perp}{m_p}\gamma^- , \tag{21}$$

where $f_1(x, k_\perp)$ is the unpolarized TMD and $h_1^\perp(x, k_\perp)$ is the Boer-Mulders function.

$$-\frac{\epsilon^{\alpha\rho}(k_\perp)_\rho}{m_p} h_1^\perp(x, k_\perp) = \frac{1}{2}\mathrm{Tr}\left(\Phi i \sigma^{\alpha +}\gamma_5\right) . \tag{22}$$

Time-reversal operation: final (initial) state is transformed into the initial (final) state and thereby spins and momenta are reversed. $S \cdot (p_1 \times p_2)$ implies the violation of time-reversal invariance, and the quantity $s_T^i \epsilon^{ij} k_\perp^j$ is of this type. Consequently, $h_1^\perp(x, k_\perp)$ is naive time-reversal odd.

Correlation function for SIDIS in quark chirality space

Correlation function for SIDIS

$$\left(P_+\Phi(x,k_\perp)\gamma^+\right)_{ji} = \begin{pmatrix} f_1(x,k_\perp) & 0 & 0 & ie^{i\phi_p}\frac{|k_\perp|}{m_p}h_1^\perp(x,k_\perp) \\ 0 & 0 & 0 & 0 \\ 0 & 0 & 0 & 0 \\ -ie^{-i\phi_p}\frac{|k_\perp|}{m_p}h_1^\perp(x,k_\perp) & 0 & 0 & f_1(x,k_\perp) \end{pmatrix}, \tag{23}$$

and correlation matrix in good quark chirality space

$$\left(P_+\Phi(x,k_\perp)\gamma^+\right)_{\chi',\chi} = \begin{pmatrix} f_1(x,k_\perp) & ie^{i\phi_p}\frac{|k_\perp|}{m_p}h_1^\perp(x,k_\perp) \\ -ie^{-i\phi_p}\frac{|k_\perp|}{m_p}h_1^\perp(x,k_\perp) & f_1(x,k_\perp) \end{pmatrix} = \begin{pmatrix} RR & RL \\ LR & LL \end{pmatrix}. \tag{24}$$

ϕ_p: azimuthal angle of the transverse momentum vector. Consequently, $h_1^\perp(x,k_\perp)$ is chiral odd. The fact that the matrix has to be positive definite allows us to derive the positivity bound

$$\frac{|k_\perp|}{m_p}|h_1^\perp(x,k_\perp)| \leq f_1(x,k_\perp), \tag{25}$$

Constrains to Boer-Mulders function

Two constrains to Boer-Mulders function:

- Positivity bound

$$\frac{|k_\perp|}{m_\pi}|h_1^\perp(x,k_\perp)| \leq f_1(x,k_\perp)\,. \tag{26}$$

- Boer Mulders functions are all expected to be negative [Matthias Burkardt, Brian Hannafious, Are all Boer-Mulders functions alike? Phys. Lett. B 658 (2008) 130-137], which is confirmed by Lattice QCD [QCDSF/UKQCD Collaborations, The spin structure of the pion, Phys. Rev. Lett.101:122001,2008].

Correlation function for SIDIS in quark chirality space

The distribution of transversely polarized quarks in an unpolarized hadron [Barone, Niccolo Cabeo lectures 2010]

$$
\begin{aligned}
f_{q^{\uparrow}/p}(x, k_{\perp}) =& \frac{1}{2}\mathrm{Tr}\left(\Phi\frac{1}{n_{-}}\right) + \frac{1}{2}\mathrm{Tr}\left(\Phi i\sigma_{\mu\nu}\gamma_5 n_{-}^{\mu} S_q^{\nu}\right) \\
=& \frac{1}{2}\left[f_1(x, k_{\perp}) - h_1^{\perp}(x, k_{\perp})\frac{(\hat{P}\times k_{\perp})\cdot S_q}{m_p}\right],
\end{aligned} \tag{27}
$$

and from this the spin asymmetry is given

$$
f_{q^{\downarrow}/p}(x, k_{\perp}) - f_{q^{\uparrow}/p}(x, k_{\perp}) = h_1^{\perp}(x, k_{\perp})\frac{(\hat{P}\times k_{\perp})\cdot S_q}{m_p}. \tag{28}
$$

Probabilistic interpretation

$h_1^{\perp} =$ 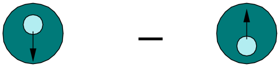

Gauge-invariant correlation function for SIDIS

The correlation function

$$\Phi(x, k_\perp) = \int \frac{d^3r}{8\pi^3} e^{-ixP^+r^- + ik_\perp\cdot r_\perp} \langle P|\bar{\psi}(0^+, r^-, r_\perp)\psi(0)|P\rangle\,, \tag{29}$$

and the gauge invariance can be restored by inserting a Wilson line

$$\Phi(x, k_\perp) = \int \frac{d^3r}{8\pi^3} e^{-ixP^+r^- + ik_\perp\cdot r_\perp} \langle P|\bar{\psi}(0^+, r^-, r_\perp)U_{(r;0)}\psi(0)|P\rangle\,. \tag{30}$$

Wilson line has to connect the point $(0^+, 0^-, 0_\perp)$ with the point $(0^-, r^+, r_\perp)$.
We first add a light-like line to each quark:

$$\begin{aligned} &U^-_{(+\infty^-, 0_\perp; 0^-, 0_\perp)}\psi(0^+, 0^-, 0_\perp)\,, \\ &\bar{\psi}(0^+, r^-, r_\perp)U^{-\dagger}_{(+\infty^-, r_\perp; r^-, r_\perp)}\,, \end{aligned} \tag{31}$$

and we then need a Wilson line to connect the transverse 'gap',

Gauge-invariant correlation function for SIDIS

$$U_{(r;0)} = U^{-\dagger}_{(+\infty^-;r^-)} U^{\perp}_{(r_\perp;0_\perp)} U^{-}_{(+\infty^-;0^-)} \,. \tag{32}$$

We split the transverse line at $+\infty_\perp$ as well. Adding this to the each quark gives

$$\begin{aligned} &U^{\perp}_{(+\infty^-,+\infty_\perp;+\infty^-,0_\perp)} U^{-}_{(+\infty^-,0_\perp;0^-,0_\perp)} \psi(0^+,0^-,0_\perp)\,, \\ &\bar\psi(0^+,r^-,r_\perp) U^{-\dagger}_{(+\infty^-,r_\perp;r^-,r_\perp)} U^{\perp\dagger}_{(+\infty^-,+\infty_\perp;+\infty^-,r_\perp)} \,. \end{aligned} \tag{33}$$

Gauge-invariant TMD correlation function

$$\begin{aligned} \Phi(x,k_\perp) &= \int \frac{d^3r}{8\pi^3} e^{-ixP^+r^-+ik_\perp\cdot r_\perp} \langle P|\bar\psi(0^+,r^-r_\perp) \widetilde{U^{\dagger}_{(+\infty;r)}} \widetilde{U_{(+\infty;0)}} \psi(0)|P\rangle \,, \\ \widetilde{U^{\dagger}_{(+\infty;r)}} &= U^{\perp}_{(+\infty^-,+\infty_\perp;+\infty^-,0_\perp)} U^{-}_{(+\infty^-,0_\perp;0^-,0_\perp)} \,, \\ \widetilde{U_{(+\infty;0)}} &= U^{-\dagger}_{(+\infty^-,r_\perp;r^-,r_\perp)} U^{\perp\dagger}_{(+\infty^-,+\infty_\perp;+\infty^-,r_\perp)} \,. \end{aligned} \tag{34}$$

Gauge-invariant correlation function for SIDIS

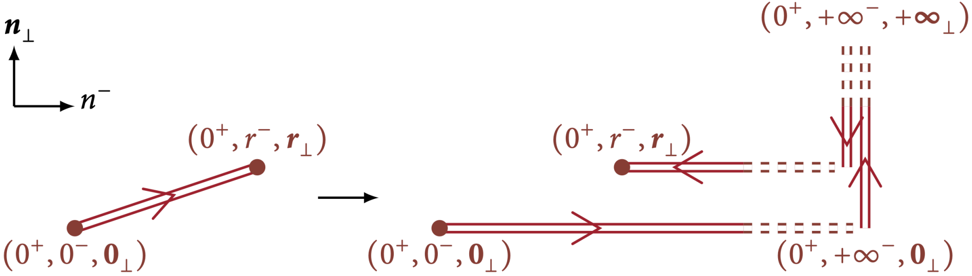

Figure: Structure of Wilson lines in the TMD definition for SIDIS.

Gauge-invariant correlation function for SIDIS

Wilson lines:

- Need to be included to ensure gauge invariance
- U^{-} and $U^{-\dagger}$: resummation of collinear gluons
- $U^{\perp}$ and $U^{\perp\dagger}$: resummation of soft transversal gluons
- Choosing light-cone gauge, only transversal Wilson lines remain
- Choosing Feyman gauge, only longitudinal Wilson lines remain
- In Drell-Yan process, Wilson line represents initial state radiation, the path of Wilson line flows towards $-\infty$ before returning. Consequently, Boer-Mulders function is T-odd and has a sign change between Drell-Yan and SIDIS processes. This also implies TMD is process-dependent.

Eikonal approximation and Wilson propagator

Eikonal approximation: a quark with momentum large enough to neglect the change in momentum due to the emission or absorption of a soft gluon.

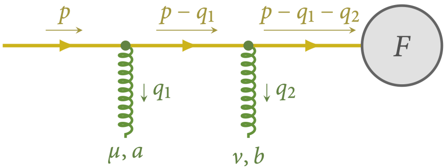

Figure: An incoming quark with momentum p radiating two soft gluons with momentum q_1 and q_2, the blob representing all possible diagrams connected to the quark propagator.

Eikonal approximation: neglecting q_1 and q_2 with respect to p.
Quark propagators will be replaced by Wilson line propagators, and quark-gluon couplings by Wilson vertices. By using the eikonal approximation, we literally factorized out the gluon contribution from the Dirac part. This remains valid when radiating more gluons.

Eikonal approximation and Wilson propagator

Feynman Rules for Linear Wilson Lines:

A. *Propagator:*

$$= \frac{\mathrm{i}}{n\cdot k + \mathrm{i}\eta},$$

B. *External point:*

$$= e^{\mathrm{i}\, a\cdot k},$$

C. *Line to infinity:*

$$= 1,$$

D. *Wilson vertex:*

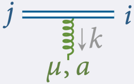

$$= \mathrm{i}\, g\, n^\mu\, (t^a)_{ij}\,.$$

Gauge-invariant correlation function

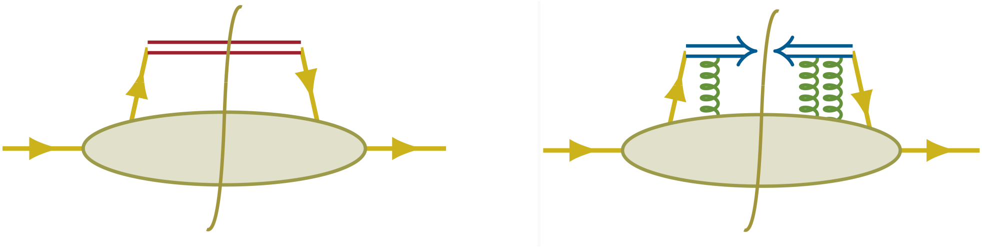

Figure: Left: gauge-invariant correlation function, with a cut Wilson line; Right: Wilson lines inside the correlation function account for the resummation of gluons.

Gauge-invariant correlation function at first order

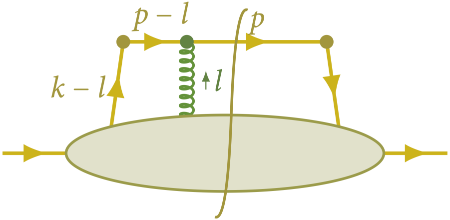

Figure: The first order diagram, where one soft gluon before the cut connects the struck quark with the blob.

The quark propagator with momentm $p-l$ need to be replaced by Wilson line propagator $\frac{i}{n\cdot(p-l)+i\eta}$, and quark gluon vertex by Wilson vertex $ign^{\mu}(t^a)_{ij}$.

Gauge-invariant correlation function at first order

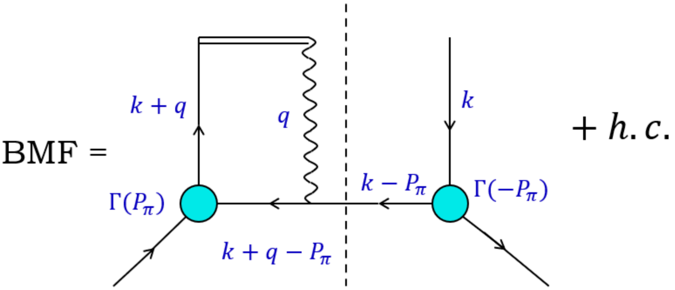

Figure: The first order diagram to calculate the Boer-Mulders fucntion. The Hermitean conjugate partner is considered.

Figure: Dan-Dan Cheng

Boer-Mulders function in contact interaction

Boer-Mulders function can be expressed as

$$\frac{2h_{1\pi}^{\perp}(x,k_\perp^2)k_\perp^\alpha}{m_\pi} = -i\int\frac{d^4q dk^-}{(2\pi)^8}\mathrm{Tr}\Big[S(k-P_\pi)\Gamma(-P_\pi)S(k)\sigma^{\alpha+}g_1 n^\mu\frac{1}{q^+ + i\epsilon}$$
$$\times S(k+q)\Gamma(P_\pi)S(k+q-P_\pi)g_2\gamma^v D_{\mu\nu}\Big] + \text{h.c.} \tag{35}$$

Contact interaction: the gluon propagator is

$$D_{\mu\nu}(k) = G(k^2)T_{\mu\nu}(k)\,, \quad G(k^2) = \frac{4\pi\alpha_{\text{IR}}}{m_G^2}\,, \quad T_{\mu\nu}(k) = \delta_{\mu\nu} - \frac{k_\mu k_\nu}{k^2}\,. \tag{36}$$

Consequently, the quark propagator and the Bethe-Salpeter amplitude are

$$S(k) = 1/[i\gamma\cdot k + M]\,, \quad \Gamma_\pi(P) = \gamma_5\left[iE_\pi(P) + \frac{1}{2M}\gamma\cdot PF_\pi(P)\right]\,. \tag{37}$$

Boer-Mulders function in contact interaction

Applying the Cutkosky rules (putting internal propagators on the mass-shell in order to determine the imaginary part of the Feynman amplitude), cutting the antiquark propagator and the Wilson line propagator:

$$\frac{1}{q^+ + i\epsilon} \to -2\pi i \delta(q^+) \,, \tag{38}$$

$$\frac{1}{(k-P_\pi)^2 + M^2 + i\epsilon} \to -2\pi i \delta\left[(k-P_\pi)^2 + M^2\right] \,. \tag{39}$$

Perform the integration over q^+ and k^- by using the two δ functions. The integration over q^- and $q_\perp$ is crucial. The result is

$$\begin{aligned} h_{1\pi}^{\perp}(x,k_\perp^2) = & \frac{3\alpha_{\mathsf{IR}} m_\pi (E_\pi - 2F_\pi)\overline{C}_2(\omega_1)}{4\pi^3 m_G^2 M} \\ & \times \left\{\left[M^2(E_\pi - F_\pi) - F_\pi x(1-x)m_\pi^2\right]\overline{C}_1(\omega_2) + F_\pi \overline{C}_0(\omega_2)\right\} \,. \end{aligned} \tag{40}$$

Boer-Mulders function in contact interaction

Useful Formulae

$$\begin{aligned}\omega_1 =& k_\perp^2 + M^2 - x(1-x)m_\pi^2\,,\\ \omega_2 =& M^2 - x(1-x)m_\pi^2\,.\end{aligned} \tag{41}$$

Incomplete gamma-functions

$$\begin{aligned}\overline{C}_1(\sigma) =& \Gamma(0,\sigma\tau_{\text{ir}}^2) - \Gamma(0,\sigma\tau_{\text{uv}}^2)\,,\\ 2\overline{C}_2(\sigma) =& \Gamma(1,\sigma\tau_{\text{ir}}^2) - \Gamma(1,\sigma\tau_{\text{uv}}^2)\,.\end{aligned} \tag{42}$$

Parameters (dimensioned quantities in GeV):

Meson	m_G	Λ_{uv}	α_{IR}	M	m_π	E_π	F_π
Pion	0.5	0.905	0.363π	0.367	0.14	3.594	0.474

Numerical results

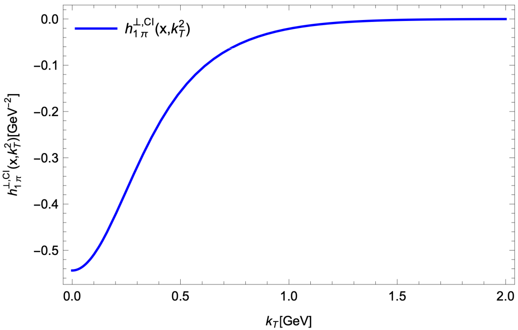

Figure: The $k_\perp$ dependence of Boer-Mulders function in contact interaction (preliminary result).

Unpolarized TMD in contact interaction

Unpolarized TMD in contact interaction [Zhang, Cui, Ping, Roberts, Eur. Phys. J. C 81 (2021) 1, 6]

$$f_1(x, k_\perp^2) = \frac{N_c}{2\pi^3}\{E_\pi(E_\pi - 2F_\pi)\overline{C}_2(\omega_1)/\omega_1 + 3\left[E_\pi^2 - 4E_\pi F_\pi + 4F_\pi^2\right] \times x(1-x)m_\pi^2 \overline{C}_3(\omega_1)/\omega_1^2\}\,, \quad (43)$$

with

$$\overline{C}_3(\sigma) = \frac{1}{6}[\Gamma(2, \sigma\tau_{\text{uv}}^2) - \Gamma(2, \sigma\tau_{\text{ir}}^2)]\,. \quad (44)$$

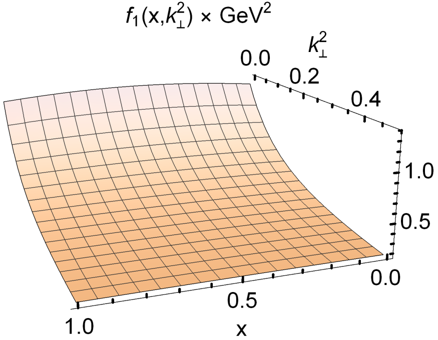

Quark-spectator-antiquark model adding dipole form factor

Pion-quark-antiquark coupling vertex is a constant coupling g_π (point-like), which yields

$$h_{1\pi}^{\perp}(x, k_\perp) = \frac{A_\pi(x)}{k_\perp^2 [k_\perp^2 + B_\pi(x)]} \ln \left[\frac{k_\perp^2 + B_\pi(x)}{B_\pi(x)} \right] , \tag{45}$$

Adding a dipole form factor to the vertex [Lu, Ma, Phys. Lett. B 615 (2005) 200-206], phenomenologically suppress the influence of high $k_\perp$, and eliminate the logarithmic divergences:

$$g_\pi(k^2) = N_\pi \frac{k^2 - M^2}{(\Lambda^2 - k^2)^2} = N_\pi (1-x)^2 \frac{k^2 - M^2}{\left[k_1^2(x,k) + L_\pi^2(x)\right]^2} , \tag{46}$$

which yields

$$h_{1\pi}^{\perp}(x, k_\perp) = \frac{|e_1 e_2|}{4\pi} \frac{N_\pi^2 (1-x)^3 M m_\pi}{2(2\pi^3) L_\pi^2(x) \left[k_\perp^2 + L_\pi^2(x)\right]^3} . \tag{47}$$

Generalized Boer-Mulders shift

[M. Engelhardt, P. Hagler, B. Musch, J. Negele and A. Schafer, Lattice QCD study of the Boer-Mulders effect in a pion, Phys. Rev. D 93, 054501 (2016)]

$$\langle k_y \rangle_{UT}(b_T^2) \equiv m_\pi \frac{\tilde{h}_1^{\perp[1](1)}(b_T^2)}{\tilde{f}_1^{[1](0)}(b_T^2)} , \qquad (48)$$

where $\tilde{h}_1^{\perp[1](1)}(b_T^2)$ and $\tilde{f}_1^{[1](0)}(b_T^2)$ are x-moments of generic Fourier-transformed TMDs:

$$\tilde{f}^{[m](n)}(b_T^2) = n! \left(-\frac{2}{m_\pi^2} \partial_{b_T^2} \right)^n$$
$$\int_{-1}^{1} dx\, x^{m-1} \int d^2k_T\, e^{ib_T \cdot k_T}\ f(x, k_T^2) \quad (49)$$

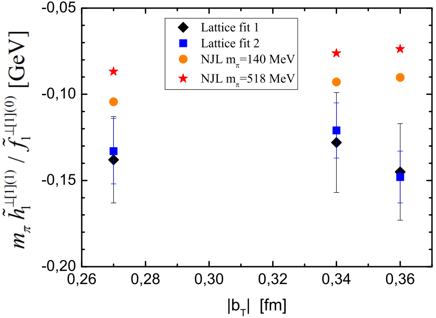

Beyond one-gluon exchange

- Include final-state interactions (FSIs) between re-scattered eikonalized quark and antiquark
- the FSIs are described by a non-perturbative scattering amplitude M that is calculated in a generalized ladder approximation
- Gluon interactions as shown in the second diagram are not taken into account. [Leonard Gamberg, Marc Schlegelc, Final state interactions and the transverse structure of the pion using non-perturbative eikonal methods, Phys. Lett. B 685: 95-103, 2010]

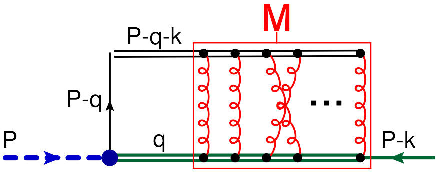

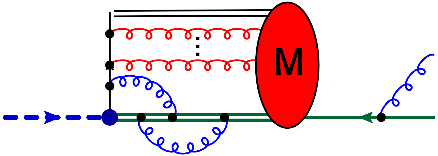

Summary and Outlook

Summary

- Pion parton distribution function
  Experiments: JLab, COMPASS++/AMBER, EIC and EicC;
  Global fits;
  Continuum methods and Lattice QCD
- Boer-Mulders function
  Gauge-invariant correlation function for SIDIS, Wilson line, transverse one, path-dependent, process-dependent, Eikonal approximation and Wilson propagator, resummation of gluons, one gluon exchange diagram, contact interaction

Outlook

- Overlap representation
- Evolution of TMDs


Thank you!